

The nature of the continuum limit in the 2D RP^2 gauge model

S.M. Catterall, M. Hasenbusch, R.R. Horgan, R. Renken

December 2, 2024

Abstract

The RP^2 gauge model which allows interpolation between the RP^2 and $O(3)$ spin models is studied in 2D. We use Monte-Carlo renormalization techniques for blocking the mean spin-spin interaction, $\langle A \rangle$, and the mean gauge field plaquette, $\langle P \rangle$. The presence of the $O(3)$ renormalized trajectory is verified and is consistent with the known three-loop β -function. The first-order ‘vorticity’ transition observed by Solomon et al. [?] is confirmed, and the location of the terminating critical point is established. New scaling flows in $(\langle A \rangle, \langle P \rangle)$ are observed associated with a large exponent κ in the range $4 \sim 5$. The scaling flows are found to give rise to a strong cross-over effect between regions of high and low vorticity and are likely to induce an apparent signal for scaling in the cross-over region which we propose explains the scaling observed for RP^2 and RP^3 models [?] and also in a study of the $SO(4)$ matrix model [?]. We show that the signal for this ‘pseudo’ scaling will occur for the RP^2 spin model in the cross-over region which is precisely the region in which computer simulations are done. We find that the RP^2 spin model is in the same universality class as the $O(3)$ spin model but that it is likely to require a very large correlation length before the true scaling of this class sets in. We conjecture that the scaling flows are due either to the influence of a nearby new renormalized trajectory or to the ghost of the Kosterlitz-Thouless trajectory in the associated XY model. In the former case it is argued that the ‘vorticity’ fixed point controlling the critical behaviour terminating the first-order line cannot be identified with the conjectured new renormalized trajectory.

1 Introduction

The nature of the phase diagram for two-dimensional RP^N models has been the subject of much recent discussion [?], [?]. In [?], Caracciolo et al. compare the correlation length computed from simulation with that predicted from the perturbative β -function using the exact results for the mass gap in $O(N)$ models. They found that for RP^2 (RP^3) the observed correlation length on lattices up to $L = 512$ was smaller than the expected value by a factor of 10^7 (10^4). Their conclusion was that either the asymptotic regime is very far indeed removed from the regime of their study, requiring lattices of sizes of 10^9 (10^5), or that these theories were not asymptotically free but that there exists a phase transition at finite β (non-zero temperature). Caracciolo et al. indeed provide evidence for the latter scenario by showing that their data scale in a manner consistent with a Kosterlitz-Thouless parametrization. The two persuasive features are thus that the correlation length is much smaller than that expected assuming an asymptotically free theory and that scaling of the data is observed. This phenomenon occurs in a large class of models and the question is whether the signal for a phase transition at finite β and the observed scaling of data are genuine or not.

The same effects have been observed to a less extreme extent by Hasenbusch and Horgan [?] who investigated the continuum limit of the $SO(4)$ matrix model. The measured ratio of the mass gap to $\Lambda_{\overline{MS}}$ was compared with the theoretical prediction obtained using the Bethe ansatz [?]. There was a disagreement between theory and experiment by about a factor of four the measured correlation length being about four times smaller than expected. However, the measurement using the covering group was in excellent agreement with theory. The numerical method used, due to Lüscher et al. [?], relies in part on measuring the correlation length in a large volume and establishing that scaling holds with only small and perturbative violations. Although in the $SO(4)$ case there were strong indications that the results scaled, the discrepancy between simulation and theory led to the conclusion that the signal for scaling was only apparent and that a true continuum limit had not been achieved in the large volume simulation. It was conjectured that the cause of the deception was the presence of vortices in the $SO(4)$ model which are absent in the case of the covering group since

$$\Pi_1(SO(4)) = Z_2, \quad \Pi_1(SU(2)) = 0. \quad (1.1)$$

One question is, therefore, whether a bogus signal for scaling can be observed in the presence of vortices in two dimensions. In the work presented here this question is addressed in the context of an RP^2 gauge theory which allows an interpolation between the pure RP^2 and $O(3)$ spin models. This gauge model contains Z_2 vortices coupled to a chemical potential. We observe the conventional $O(3)$ renormalized trajectory and show that our results are consistent with the known three-loop β function. We establish the existence of a first-order transition, first suggested by Solomon et al. [?], for which the order parameter is the vorticity. The critical point terminating this first-order line will be in the domain of a new ‘vorticity’ fixed point. Using Monte-Carlo renormalization group (MCRG) techniques we observe certain flows on which the blocked observables scale and suggest that these scaling flows are due to the influence of a nearby renormalized

trajectory which gives rise to the possibility of the existence of a fixed point other than the $O(3)$ one. We argue that it is unlikely that any new fixed point can be identified with the inferred ‘vorticity’ fixed point. Our results strongly indicate that the apparent or ‘pseudo’ scaling behaviour is due to a cross-over effect associated with the proximity of the new scaling flows to the line of RP^2 spin models in coupling constant space. The cross-over is between regions of high and low vorticity which emphasizes the crucial rôle of vorticity in the observed properties of the model. Where relevant our results confirm or complement those obtained by Solomon et al. [?] in an earlier study of this model.

Another reason for studying the RP^2 gauge models is that it has been conjectured [?] that in 2D the continuum limit in the RP^2 spin model is distinct from that in the $O(3)$ spin model. Niedermayer et al. [?] and Hasenbusch [?] have suggested that this conjecture is incorrect and that there does exist a continuum limit in the RP^2 model which is controlled by the $O(3)$ fixed point. The essential question is whether or not the RP^2 model is in the same universality class as the $O(3)$ model. By using MCRG methods to show the topology of renormalization group trajectories in the RP^2 gauge theory we find that a consistent and simple interpretation of our results is that the RP^2 and $O(3)$ models are in the same universality class: an interpretation which supports the conclusions of Niedermayer et al. [?] and Hasenbusch [?].

All results are for RP^2 gauge models but the simulation can be generalized to RP^{N-1} and a cursory investigation for $N > 3$ has indicated that broadly similar results hold for this general case.

In section 2 we define the model under study; in section 3 we briefly describe the simulation techniques; in section 4 we define the Monte-Carlo renormalization group method used and describe the measurement procedure; in section 5 we present the results and discussion and in section 7 we draw our conclusions.

2 The model

The action used is

$$S(\{\mathbf{S}\}, \{\mathbf{s}\}) = -\beta \left(\sum_{\mathbf{x}, \boldsymbol{\mu}} \mathbf{S}_{\mathbf{x}} \cdot \mathbf{S}_{\mathbf{x}+\boldsymbol{\mu}} \sigma_{\mathbf{x}, \boldsymbol{\mu}} + \mu \sum_{\mathbf{x}} P_{\mathbf{x}}(\sigma) \right),$$

where $\mathbf{x} = (x_1, x_2)$, $x_1, x_2 \in Z$, $1 \leq x_1, x_2 \leq L$, labels the sites of an integer 2D square lattice of side L , and $\boldsymbol{\mu}$ takes values in $\boldsymbol{\mu}_1 = (0, 1)$, $\boldsymbol{\mu}_2 = (1, 0)$. The spin $\mathbf{S}_{\mathbf{x}}$ is a unit length three-component vector at site \mathbf{x} and $\sigma_{\mathbf{x}, \boldsymbol{\mu}}$ is a gauge field on the link $(\mathbf{x}, \boldsymbol{\mu})$ taking values in $[1, -1]$. The plaquette of gauge fields is denoted by $P_{\mathbf{x}}(\sigma)$ where

$$P_{\mathbf{x}}(\sigma) = \sigma_{\mathbf{x}, \boldsymbol{\mu}_1} \sigma_{\mathbf{x}+\boldsymbol{\mu}_1, \boldsymbol{\mu}_2} \sigma_{\mathbf{x}+\boldsymbol{\mu}_2, \boldsymbol{\mu}_1} \sigma_{\mathbf{x}, \boldsymbol{\mu}_2}. \quad (2.1)$$

This action is invariant under the gauge transformation

$$\begin{aligned} \mathbf{S}_{\mathbf{x}} &\rightarrow g_{\mathbf{x}} \mathbf{S}_{\mathbf{x}}, \\ \sigma_{\mathbf{x}, \boldsymbol{\mu}} &\rightarrow g_{\mathbf{x}} \sigma_{\mathbf{x}, \boldsymbol{\mu}} g_{\mathbf{x}+\boldsymbol{\mu}}, \end{aligned} \quad (2.2)$$

with $g_{\mathbf{x}} \in [1, -1]$.

Vortices reside on plaquettes where $P_{\mathbf{x}}(\sigma) = -1$, and are suppressed (enhanced) if the chemical potential, μ , is positive (negative). The pure $O(3)$ model corresponds to $\mu \rightarrow \infty$ and the pure RP^2 model corresponds to $\mu = 0$.

3 The simulation

A local update was used comprising a combination of heat-bath, microcanonical and demon schemes. For fixed gauge fields the spins $\{\mathbf{S}\}$ were first updated by a heat-bath algorithm which can be generalized to $O(N)$ and so for this section we will consider $\mathbf{S}_{\mathbf{x}}$ to be an N -component spin of unit length. The heat-bath method is to project each spin onto a 3D subspace of the N -dimensional space in which the spins take their values. The 3D subspace is chosen at random but is the same for all spins during one lattice update. Let the projection of $\mathbf{S}_{\mathbf{x}}$ onto this space be denoted $\mathbf{R}_{\mathbf{x}}$. Then clearly

$$(\mathbf{R}_{\mathbf{x}})_i = (\mathbf{S}_{\mathbf{x}})_{j_i} , \quad i = 1, 2, 3 , \quad 1 \leq j_1 < j_2 < j_3 \leq N , \quad (3.1)$$

where the j_i are chosen randomly subject to the restrictions above. The single-site probability distribution for $\mathbf{R}_{\mathbf{x}}$ is then

$$Q(\mathbf{R}_{\mathbf{x}}) \propto \exp(\mathbf{M}_{\mathbf{x}} \cdot \mathbf{R}_{\mathbf{x}}) , \quad (3.2)$$

where

$$\mathbf{M}_{\mathbf{x}} = \beta \sum_{\mu} (\mathbf{R}_{\mathbf{x}+\mu} \sigma_{\mathbf{x},\mu} + \mathbf{R}_{\mathbf{x}-\mu} \sigma_{\mathbf{x}-\mu,\mu}) . \quad (3.3)$$

The heat-bath update at each site is done by replacing $\mathbf{R}_{\mathbf{x}}$ by $\mathbf{R}'_{\mathbf{x}}$ which is chosen with the probability distribution $Q(\mathbf{R}_{\mathbf{x}})$. The microcanonical spin update is

$$\mathbf{S}_{\mathbf{x}} \rightarrow \mathbf{S}'_{\mathbf{x}} = -\mathbf{S}_{\mathbf{x}} + \frac{2(\mathbf{S}_{\mathbf{x}} \cdot \mathbf{M}_{\mathbf{x}}) \mathbf{M}_{\mathbf{x}}}{|\mathbf{M}_{\mathbf{x}}|^2} . \quad (3.4)$$

The demon update is applied to the gauge fields only. In general, it is only necessary to introduce one demon variable for the whole gauge configuration. However, when running on a massively parallel computer it is necessary to have one demon per processor and then each demon must migrate through the whole lattice. This is easily achieved by moving demons sequentially between processors. We illustrate the method with one demon variable d , $d \geq 0$. The action in equation (2) is augmented by the demon to become

$$S_{demon}(\{\mathbf{S}\}, \{\sigma\}, d) = S(\{\mathbf{S}\}, \{\sigma\}) + \beta d . \quad (3.5)$$

Then for each link (\mathbf{x}, μ) the trial gauge field update is $(\sigma_{\mathbf{x},\mu}, d) \rightarrow (-\sigma_{\mathbf{x},\mu}, d')$ where d' is chosen so that S_{demon} is unchanged. That is,

$$d' = d - 2 \sigma_{\mathbf{x},\mu} \{ \mathbf{S}_{\mathbf{x}} \cdot \mathbf{S}_{\mathbf{x}+\mu} + \mu (\sigma_{\mathbf{x},\nu} \sigma_{\mathbf{x}+\nu,\mu} \sigma_{\mathbf{x}+\mu,\nu} + \sigma_{\mathbf{x}-\nu,\nu} \sigma_{\mathbf{x}-\nu,\mu} \sigma_{\mathbf{x}-\nu+\mu,\nu}) \} , \quad (3.6)$$

where $\boldsymbol{\nu}$ is the orthogonal vector to $\boldsymbol{\mu}$. The update is accepted only if $d' \geq 0$. Note that the update is microcanonical in the augmented configuration space of fields plus demon and hence it is independent of β .

One complete lattice update consisted of one heat-bath update followed by an alternating sequence of N_{MD} microcanonical and demon updates. The value of N_{MD} that optimizes the decorrelation of the configurations depends on many factors and we did not spend much effort in tuning N_{MD} but regard $N_{MD} \approx 10$ as a reasonable value. The heat-bath update took about ten times the time of the combined microcanonical and demon updates and so there was little time penalty for this choice. Depending on the coupling constant values we found that decorrelated configurations were produced within 2-30 iterations. Lattice sizes ranged from 64^2 to 512^2 , and typically the numbers of configurations per run were e.g., $2 \cdot 10^6$ for 64^2 and $5 \cdot 10^5$ for 256^2 .

The simulations were carried out on the HITACHI SR2201 computers in the Cambridge High Performance Computing Facility and in the Tokyo Computing Centre.

4 The Monte-Carlo renormalization scheme

The objective is to establish the topology of renormalization group flows in the relevant large-scale variables and infer the phase structure of the model. After sufficient blocking we assume that we are dealing with renormalized observables, and so different phases will be distinguished by singularities in the renormalization group flows. This has been discussed, for example, by Nienhuis and Nauenberg [?] and by Hasenfratz and Hasenfratz [?]. We assume that there are at most two relevant couplings in the neighbourhood of any fixed point in which we are interested. We also assume that the chosen blocked operators have components which span the two-dimensional space of relevant operators, i.e., the operators conjugate to these relevant couplings. From our earlier experience [?] and from the surmise stated in the introduction that vorticity plays a vital rôle, we chose to study how the mean values of the spin-spin interaction, A , and of the plaquette, P , flow under blocking. For a given configuration these quantities are defined by

$$\begin{aligned} A &= \frac{1}{2V} \sum_{\mathbf{x}, \boldsymbol{\mu}} \mathbf{S}_{\mathbf{x}} \cdot \mathbf{S}_{\mathbf{x}+\boldsymbol{\mu}} \sigma_{\mathbf{x}, \boldsymbol{\mu}} , \\ P &= \frac{1}{V} \sum_{\mathbf{x}} P_{\mathbf{x}}(\sigma) . \end{aligned} \tag{4.1}$$

$\langle A \rangle$ lies in $[0, 1]$ and $\langle P \rangle$ lies in $[-1, 1]$ and the mean vorticity is defined by $\mathcal{V} = (1 - P)/2$.

For each configuration $\{\mathbf{S}, \sigma\}$ on a lattice of side L we derive a blocked configuration $\{\mathbf{S}^B, \sigma^B\}$ on a lattice of side $L/2$. The blocking transformation for the spins is

$$\mathbf{S}_{\mathbf{x}_B}^B = \frac{\mathbf{S}_{\mathbf{x}} + \alpha \left(\mathbf{S}_{\mathbf{x}+\boldsymbol{\mu}_1} \sigma_{\mathbf{x}, \boldsymbol{\mu}_1} + \mathbf{S}_{\mathbf{x}+\boldsymbol{\mu}_2} \sigma_{\mathbf{x}, \boldsymbol{\mu}_2} + \mathbf{S}_{\mathbf{x}-\boldsymbol{\mu}_1} \sigma_{\mathbf{x}-\boldsymbol{\mu}_1, \boldsymbol{\mu}_1} + \mathbf{S}_{\mathbf{x}-\boldsymbol{\mu}_2} \sigma_{\mathbf{x}-\boldsymbol{\mu}_2, \boldsymbol{\mu}_2} \right)}{|\text{numerator}|} .$$

(4.2)

Based on earlier work by Hasenbusch et al. [?] the parameter α was chosen to be 0.0625. Choosing other reasonable values for α was found not to change any outcome or conclusion. This gauge-invariant blocking transformation is shown in figure 1.

To block the gauge field the products of gauge fields were computed for the three Wilson lines joining the end points of the blocked link shown in figure 1. These field products are denoted by W_0, W_+, W_- . For the blocked link joining \mathbf{x} to $\mathbf{x} + 2\boldsymbol{\mu}$ the W_i are given by

$$\begin{aligned} W_0 &= \sigma_{\mathbf{x}, \boldsymbol{\mu}} \sigma_{\mathbf{x}+\boldsymbol{\mu}, \boldsymbol{\mu}} , \\ W_+ &= \sigma_{\mathbf{x}, \boldsymbol{\nu}} \sigma_{\mathbf{x}+\boldsymbol{\nu}, \boldsymbol{\mu}} \sigma_{\mathbf{x}+\boldsymbol{\mu}+\boldsymbol{\nu}, \boldsymbol{\mu}} \sigma_{\mathbf{x}+2\boldsymbol{\mu}, \boldsymbol{\nu}} , \\ W_- &= \sigma_{\mathbf{x}-\boldsymbol{\nu}, \boldsymbol{\nu}} \sigma_{\mathbf{x}-\boldsymbol{\nu}, \boldsymbol{\mu}} \sigma_{\mathbf{x}+\boldsymbol{\mu}-\boldsymbol{\nu}, \boldsymbol{\mu}} \sigma_{\mathbf{x}+2\boldsymbol{\mu}-\boldsymbol{\nu}, \boldsymbol{\nu}} , \end{aligned} \quad (4.3)$$

where $\boldsymbol{\nu}$ is the orthogonal vector to $\boldsymbol{\mu}$. The blocked gauge field was assigned the majority sign of the W_i :

$$\sigma_{\mathbf{x}_B, \boldsymbol{\mu}_B}^B = \frac{W_+ + W_0 + W_-}{|W_+ + W_0 + W_-|} . \quad (4.4)$$

This blocking transformation has the important property that it ensures that two vortices on adjacent plaquettes of the original lattice will cancel and not survive in the blocked lattice. This is clearly true if the vortices lie in the same 2×2 block since they add mod₂, but the majority rule guarantees cancellation also when two adjacent vortices lie either side of the block link separating two neighbouring blocks. This is illustrated in figure 2.

For a given pair of coupling constants (β, μ) and given lattice size $L \times L$, each configuration was blocked by successive transformations until the blocked lattice size was 8×8 . The operator expectations $\langle A \rangle_L(\beta, \mu)$ and $\langle P \rangle_L(\beta, \mu)$ were then measured and averaged over all configurations. For given (β, μ) this was done for $L = 64, 128, 256, 512$ which gives four points on a segment of a flow in the $(\langle A \rangle, \langle P \rangle)$ plane with each point labelled by initial lattice size. Each point corresponds to a rescaling of length by a factor of two compared with the previous point.

The errors on the observables were determined by averaging the results for successive configurations in bins of 2^M , $M = 0, 1, 2, \dots$ and calculating the errors on the ensemble of bin-averaged measurements [?]. The true error is the asymptotic value achieved for large enough M . The decorrelation length can also be estimated from the behaviour of the error as a function of M . The number of independent configurations ranged from about 600 for $L = 512$ to in excess of $2 \cdot 10^4$ for $L = 64$. Errors were also estimated from the ensemble of independent measurements from different processors.

5 Results

Each flow segment consisting of four points, but more complete flows can be built up by extending the flow in either direction by tuning to new couplings (β', μ')

so that

$$\begin{aligned}\langle A \rangle_{L'}(\beta', \mu') &= \langle A \rangle_L(\beta, \mu) , \\ \langle P \rangle_{L'}(\beta', \mu') &= \langle P \rangle_L(\beta, \mu) ,\end{aligned}\tag{5.1}$$

for some L and L' . The flow for given (β', μ') can then be computed. In general this will be an approximate procedure because a segment in the $(\langle A \rangle, \langle P \rangle)$ plane is the projection onto this plane of part of a full flow in the higher dimensional space of observables. By tuning as described we are ensuring only that the projections of blocked points coincide not the blocked points themselves. In principle, we need to match a full complement of observables by tuning a complete set of couplings, conjugate to these observables, which define the most general action consistent with the symmetry. In general, the effect of couplings which are not included cannot be properly taken into account. However, we assume that in the neighbourhood of a fixed point there will be at most two relevant couplings and that the projection onto the (β, μ) plane of the space they span is non-singular. The effect of irrelevant couplings is mitigated by performing an initial blocking by a factor which will significantly reduce the errors induced by the projection so that we are effectively dealing with renormalized operators. Since the target lattice is always 8×8 the size of this factor depends on the initial lattice size and hence on available CPU. For our study this initial blocking factor had a minimum value of eight.

There are errors due to finite-size effects which can be parametrized in terms of the parameter $z = \xi_L/L$ where ξ_L is the correlation length on the $L \times L$ lattice. Because the target lattice is the same size throughout, the values of z associated with coinciding points, equation (5.1), are similar and so the mismatch in the finite-size errors between different segments joining up to make a longer flow will be minimized. There will nevertheless be a residual finite-size effect which it is generally not possible to estimate except in the case of the $O(3)$ spin model which is discussed in the next section.

The details of the flows can depend on z and the details of the blocking scheme. It follows that conclusions about the physical properties of the theory can be deduced only from universal or topological properties of the flows such as the occurrence of fixed points and singular behaviour.

5.1 The $O(3)$ renormalized trajectory

In the limit $\mu \rightarrow \infty$ we recover the $O(3)$ spin model, and to test our procedures and assumptions we should, at the very least, be able to recover the perturbative β -function for this model. The projection of the $O(3)$ renormalized trajectory onto the (β, μ) plane is the β -axis. We expect corrections to scaling due to finite lattice-spacing artifacts which will be a function of L . We find that our method works well for sufficiently large β once the tree-level approximation for these scaling corrections has been taken into account. Consider the block observable $A^B = \mathbf{S}_{x_B}^B \cdot \mathbf{S}_{y_B}^B$ with the blocking transformation defined in equation 4.2. For large β we write

$$\mathbf{S}_x = q\sqrt{1 - \beta^{-1}\phi_x^2} + \beta^{-1/2}\phi_x ,\tag{5.1.1}$$

where $\mathbf{q} = (1, 0, 0)$ and $\boldsymbol{\phi} = (0, \phi_1, \phi_2)$. Using 4.2 and keeping terms up to β^{-1} we find after one blocking step that

$$\mathbf{S}_{\mathbf{x}_B}^B = \mathbf{q} \sqrt{1 - \beta^{-1} \boldsymbol{\Phi}_{\mathbf{x}_B}^2} + \beta^{-1/2} \boldsymbol{\Phi}_{\mathbf{x}_B} , \quad (5.1.2)$$

with

$$\boldsymbol{\Phi}_{\mathbf{x}_B} = \frac{\boldsymbol{\phi}_{\mathbf{x}} + \alpha \sum_{\boldsymbol{\mu}} \boldsymbol{\phi}_{\mathbf{x}+\boldsymbol{\mu}}}{1 + 4\alpha} , \quad (5.1.3)$$

and where $\boldsymbol{\mu}$ is summed over nearest neighbour links. For large β we expect the blocked expectation value, $\langle A \rangle_L$, on the 8×8 lattice to behave as

$$\langle A \rangle_L = 1 - C(L)/\beta + O(1/\beta^2) . \quad (5.1.4)$$

For large enough L we expect $C(L)$ to attain its limiting value. However, there is still some variation in $C(L)$ for the values of L we are using. In order to accommodate the bulk of this correction to scaling we define the effective coupling β_{eff} by

$$\beta_{eff}(L, \beta) = \frac{C(L)}{(1 - \langle A \rangle_L(\beta))} , \quad (5.1.5)$$

and modify the matching condition of equation (5.1) in this case to become

$$\beta_{eff}(L, \beta) = \beta_{eff}(L', \beta') . \quad (5.1.6)$$

We then expect that

$$\log(L/L') = \int_u^{u'} \frac{du}{\beta(u)} , \quad (5.1.7)$$

where $u = 1/\beta$, $u' = 1/\beta'$.

$C(L)$ is determined from a free field theory calculation on an L^2 lattice of the kinetic term for the blocked field $\boldsymbol{\Phi}_{\mathbf{x}}$ which is defined on the target L_B^2 lattice by iteration of equation (5.1.3). This calculation is done easily numerically and the results are given in table 1. We use $L_B = 8$ in subsequent calculations.

L	$C(L, L_B = 8)$	$C(L, L_B = 4)$
16	0.53890071	0.54363018
32	0.56795927	0.55935100
64	0.58370587	0.56866918
128	0.59303041	0.57453025
256	0.59889307	0.57829938
512	0.60266260	0.58074276

Table 1: The function $C(L)$ defined in equation (5.1.4) for blocking from an L^2 lattice for target lattices with $L_B = 8, 4$. $C(L)$ gives the tree approximation for the dependence on L/a of corrections to scaling in the $O(3)$ spin model.

Using equation (5.1.7) and the three-loop β -function from [?] we determine sequences for the bare coupling, β , for which successive terms correspond to blocking by a factor of two. In table 2 we compare the values of β_{eff} for the

two sequences $\beta = 5.0, 4.8861, 4.7721$ and $2.0, 1.8803, 1.7560$. If our simulation reproduces the correct β -function then the matching condition

$$\beta_{eff}(2^{(m-n)}L, \beta_n) = \beta_{eff}(L, \beta_m) , \quad (5.1.8)$$

must be satisfied, where β_n is the n -th term in the sequence. From table 2 we see that this condition is indeed very well satisfied for the sequence starting with $\beta = 5.0$. For the other sequence the larger values of β_{eff} agree well and only as β_{eff} decreases is there an increasing discrepancy which signals a significant deviation of the three loop approximation to the β -function from the correct value and also the possible effect of the neglected L -dependent $O(1/\beta^2)$ terms in equation (5.1.5). Our expectation is confirmed that the method correctly reproduces asymptotic scaling and probes the renormalization group flow close to the renormalized trajectory.

β	Initial lattice size, L			
	64	128	256	512
5.0	–	4.355(1)	4.227(3)	4.107(5)
4.8861	4.343(1)	4.244(3)	4.110(3)	3.995(5)
4.7721	4.249(1)	4.124(1)	4.002(3)	–
2.0	–	1.2752(4)	1.1366(4)	0.9852(7)
1.8803	1.2733(2)	1.1289(4)	0.9729(7)	0.8194(4)
1.7560	1.1210(3)	0.9532(4)	0.8000(2)	–

Table 2: Values of $\beta_{eff}(L, \beta)$ for sequences of bare coupling β computed using equation (5.1.7) where successive couplings in the sequence correspond to blocking by a factor of two. The required matching condition, equation (5.1.8), for verification of asymptotic scaling is very well satisfied for the sequence at larger β and the deviation in the other sequence is largest for the smaller values of β and is due to deviation of the three-loop approximation to the β -function from the true value and possibly to terms neglected in equation (5.1.5) .

5.2 New scaling flows

In figures 3 to 9 we plot the flow segments for various (β, μ) values in the $(\langle A \rangle, \langle P \rangle)$ plane, where the longer flows in figures 3 and 4 are composed of superimposing segments using equation (5.1). There is a flow on which the observables scale. This is shown in figures 3 and 4. Nearby flows also showed scaling but are not included in the figures for reasons of clarity. To see that observables scale each flow of four points was successively overlaid using the tuning described in equation (5.1) with $L' = L/2$. For the scaling flows the points of the overlaid flow segments coincide very well within errors (the tuning is not absolutely exact) showing that there are only very small effects from the irrelevant operators. In table 3 we give the values of $(\langle A \rangle, \langle P \rangle)$ for points on the segments making up two such scaling flows, labelled set 1 and set 2, together with the initial lattice sizes and coupling constant values.

The tuning described by equation (5.1) was done by trial and error. We tried to estimate the effect of small increments in the coupling constant values by using the method of reweighting but this was found not to work. This was mainly because the blocked $(\langle A \rangle, \langle P \rangle)$ values were very sensitive to the initial couplings and so to use reweighting was not a realistic possibility. Also it was found that the effect of a change in β could be partly compensated by a change in μ . This was because the Jacobian $\partial(\langle A \rangle, \langle P \rangle)/\partial(\beta, \mu)$ was relatively small and presumably a better choice for the pair of observables and/or initial couplings would increase its value. However, in no case was this Jacobian dangerously small and tuning by trial was effective.

For these flows we did not apply a compensation for scaling corrections of the kind used in the previous section for the $O(3)$ model. It is not possible to carry out a similar tree-level calculation to determine the compensation, if any, as a function of L/a since the model and the appropriate coupling(s) associated with the scaling flows are not known. Also, the data presented in this section were obtained before the details of the $O(3)$ analysis were known and the possible residual dependency on L analyzed. Overall, the deviation from scaling for the scaling flows is not large and we must allow for the possibility that it is due, in some measure, to the finite lattice-spacing artifact of the kind analyzed for $O(3)$. However, there are a few points shown which do deviate substantially from scaling for which such an explanation is unlikely. For both sets these points are for the two largest values used for β , and for the largest initial lattice size, $L = 512$. We defer the discussion of the reasons why they do not scale well until section 6.

For the couplings which generate the scaling flow denoted by set 1, a plot of $\exp(-\mu)$ versus $g = 1/\beta$ can be approximated by a straight line with all except the one with smallest β well fitted by

$$\exp(-\mu) = 1.74(1) - 2.98(4)g, \quad (5.2.1)$$

Phenomenologically, we find that it is consistent to associate a scaling exponent, κ , with the scaling flow using the relation

$$\kappa = p \log(2) / \log((g_1 - g^*)/(g_2 - g^*)) . \quad (5.2.2)$$

where the number of blockings for g_1 and g_2 differ by p (a factor of 2^p in change of scale) in order for the corresponding points in the $(\langle A \rangle, \langle P \rangle)$ plane to coincide on the scaling flow. The value of g^* is a free parameter which is chosen to obtain the best fit assuming κ in equation (5.2.2) is constant. Even so, g^* is not very well determined by this alone and we find a range of values $g^* \approx .13 \sim .15$ to be acceptable, for which the various pairings of couplings for set 1 from table 3 give the values for κ shown in table 4. The values of μ^* in table 4 are inferred using the linear fit of equation (5.2.1). Note that the possible values of μ^* in table 4 are far removed from the value $\mu = 0$ which characterizes the RP^2 model. Taking κ in the range $4 \sim 5$, the dimension of the relevant operator associated with the scaling flows is

$$\Delta = D - 1/\kappa \approx 1.75 \sim 1.8 . \quad (5.2.3)$$

A word of caution. The definition of κ used in equation (5.2.2) is appropriate for conventional second-order behaviour. However, the consistency of the fit

	(β, μ)	Initial lattice size, L			
		64	128	256	512
Set 1	4.26, -0.045	0.81894(3)	0.80587(9)	0.7913(2)	0.7761(3)
		0.98330(4)	0.9809(2)	0.9753(3)	0.9684(8)
	4.0, 0.0	0.80793(3)	0.7913(2)	0.7690(2)	0.739(1)
		0.98021(6)	0.9740(3)	0.9561(4)	0.927(3)
	3.72, 0.06	0.79261(5)	0.7678(1)	0.7273(4)	0.6424(8)
		0.97402(9)	0.9547(2)	0.9053(8)	0.770(3)
	3.45, 0.125	0.76947(6)	0.7251(2)	0.6363(4)	0.4995(6)
		0.9576(1)	0.9025(4)	0.7601(10)	0.558(1)
	3.18, 0.187	0.7233(2)	0.6298(2)	0.4872(2)	0.2878(5)
		0.9025(4)	0.7528(4)	0.5430(4)	0.3348(5)
Set 2	4.00, 0.02	0.81574(3)	0.80228(6)	0.7871(2)	0.7694(9)
		0.98787(5)	0.9849(1)	0.9782(4)	0.967(2)
	3.73, 0.0833	0.80236(4)	0.7846(1)	0.7611(2)	0.720(1)
		0.98518(6)	0.9768(2)	0.9571(5)	0.905(3)
	3.495, 0.14	0.78475(7)	0.7577(1)	0.7085(3)	0.611(2)
		0.9769(1)	0.9538(3)	0.8865(7)	0.727(3)
	3.3, 0.18	0.7596(1)	0.7070(1)	0.6062(4)	0.4564(7)
		0.9544(2)	0.8826(3)	0.7178(8)	0.506(1)
	3.06, 0.23	0.7050(3)	0.6002(30)	0.448(5)	0.2383(2)
		0.8821(7)	0.7105(7)	0.4990(9)	0.2973(4)

Table 3: Values of the blocked observables ($\langle A \rangle, \langle P \rangle$) for the flow segments constituting two neighbouring scaling flows labelled by set 1 and set 2. The values of the couplings (β, μ) labelling each segment is given and the different points on a given segment are labelled by the initial lattice size L . The blocked observables were measured after blocking to a fixed target lattice size of 8×8 . Scaling of the blocked observables can be seen to hold extremely well for each set by noting that the ($\langle A \rangle, \langle P \rangle$) values lying on any given diagonal sloping from bottom left to top right agree very closely indeed, except for the largest two values of β for $L = 512$. Set 1 is shown in figures 3 and 4.

should be taken only as a phenomenological parametrization and it is likely that a different scaling form such as derived from Kosterlitz-Thouless behaviour would give an equally good fit. For example, in [?] Seiler et al. study the $Z(10)$ model in 2D which they presume has a KT transition. They find that both second-order and KT scaling forms give equally good fits near the transition and that, indeed, the KT form is hard to reconcile with conventional theory.

5.3 The first-order transition

Solomon et al. [?] use simple arguments to suggest that a line of first-order transitions occur in the range $\mu_1 < \mu(\beta) < \mu_2$, $\mu_1 = -0.293$, $\mu_2 \approx -0.26$. This line of transitions will terminate in a critical point associated with a continuous transition implying that a critical surface intersects the (β, μ) coupling constant plane. Confirmation of the first-order transition is shown in figures 5 and 6 where,

(g^*, μ^*)	Scaling exponent κ									
0.13, -0.305	5.10	4.92	4.919	4.90	4.76	4.83	4.84	4.91	4.88	4.84
0.15, -0.261	4.19	4.10	4.15	4.18	4.02	4.13	4.18	4.25	4.26	4.28

Table 4: The scaling exponent κ calculated using equation (5.2.2) and various pairings of couplings $g = 1/\beta$ from set 1 given in table 3. Two different choices for (g^*, μ^*) are used which correspond to the range giving consistent results for κ .

respectively, the values of $\langle A \rangle$ and $\langle P \rangle$ for a lattice of $L = 128$ are shown plotted against μ for fixed $\beta = 6.0, 7.0, 7.5, 8.0$. It is clear that there is no transition for $\beta = 6.0, 7.0$ but that there is likely to be a first-order transition for $\beta = 7.5, 8.0$. This places the critical point in the range $7.0 < \beta^* < 7.5$ which is consistent with the investigation of Solomon et al. [?]. The value of μ^* varies a little but is close to -0.26 . There is no detectable dependence on L and studies on lattices with $L = 256, 512$ have shown identical results within statistical errors. From figures 5 we infer that a good order-parameter distinguishing the two phases is the vorticity. There is also a discontinuity in $\langle A \rangle$ shown in figure 6 which is, however, not independent of the discontinuity in $\langle P \rangle$. The value of $\langle A \rangle$ will vary rapidly since it is sensitive to, and thus reflects, the discontinuous change in the vorticity. The effective potential will show no discontinuity and it is crude but reasonable to suppose that one particular linear combination of A and P plays this rôle. In figure 7 we plot $\langle P \rangle$ against $\langle A \rangle$ and indeed it can be seen that there is no sign of a sharp discontinuity and that the locus of points is reasonably linear. The outcome is that the combined operator

$$U_C(\mathbf{x}) = \sum_{\mu} \mathbf{S}_{\mathbf{x}} \cdot \mathbf{S}_{\mathbf{x}+\mu} \sigma_{\mathbf{x},\mu} + \gamma P_{\mathbf{x}}(\sigma), \quad (5.3.1)$$

with $\gamma \approx -0.29$, has a continuous expectation value across the transition. The orthogonal combination, $U_D(\mathbf{x})$, has a discontinuous expectation value which is sensitive to the vorticity and is a good order-parameter. The simple and persuasive argument of Solomon et al. [?] is based on minimizing the energy at $\beta = \infty$ to show that a first-order transition occurs in $\langle P \rangle$ at $\mu(\infty) = 1/\sqrt{2} - 1$. The argument also depends on continuity of the energy which, at $\beta = \infty$, means that $U_C(\mathbf{x})$ is identified with the local energy operator. This will be only approximate for $\beta < \infty$.

The critical point terminating the first-order line will be in the domain of a fixed point, the ‘vorticity’ fixed point, with a renormalized trajectory on which the vortex density scales thus defining a new continuum theory with non-zero vortex density.

5.4 Cross-over of flows

In figures 8 and 9 there are two further sets of flow segments, sets 3 and 4, which each show a clear cross-over as a function of initial couplings. Set 3 lies to the left of set 4. These two sets are examples of the cross-over effect which we infer

occurs in a narrow region formed by the neighbourhood of a continuous line of theories in the (β, μ) plane.

The couplings associated with sets 3 and 4 are listed in table 5 where, for each set, the couplings reading from left to right label the segments in order from the lowest in the figure (lowest $\langle P \rangle$) to the highest (highest $\langle P \rangle$).

	(β, μ)					
Set 3	3.3 0.34	3.3 0.36	3.3 0.40	3.3 0.45	3.3 0.50	3.3 0.60
Set 4	3.9 0.0	4.05 0.0	4.17 0.0	4.19 0.0	4.29 0.0	4.5 0.0

Table 5: The couplings associated with sets 3 and 4. For each set, the couplings reading from left to right label the segments in order from the lowest in the figure (lowest $\langle P \rangle$) to the highest (highest $\langle P \rangle$).

We concentrate in particular on the flow segments of set 4 which correspond to the RP^2 spin model ($\mu = 0$). These segments are shown for various β in the range 3.9 – 4.5 where the cross-over in the flows is very strongly marked, occurring between $\beta = 4.17$ and $\beta = 4.19$. The values of $(\langle A, \rangle, \langle P, \rangle)$ blocked from $L = 64 \rightarrow L = 8$ show little variation in values but when blocked from larger L the variation is very strong indeed. Moreover, it is clear that for $\beta = 3.9 \sim 4.1$ the flow is dominated by the proximity of the scaling flows, represented as the dashed line in the figure, which will induce a signal for scaling in pure RP^2 when $\beta \sim 4$. However, as β is increased there is a strong crossover effect, and for $\beta > 4.25$ the flow is consistent with dominance by the renormalized trajectory associated with the asymptotically free $O(3)$ fixed point at $(\beta^*, \mu^*) = (\infty, \infty)$. Consequently, the apparent scaling signal will only be transitory. For finite β there will always be some free vortices, but for $\beta > \beta_{cross-over}$ we expect that the density of free vortices will vanish faster than $1/\xi^2$ and the vortex density will not scale. This behaviour is consistent with the absence of a phase transition at finite β as well as with the $O(3)$ type continuum limit in RP^2 .

6 Discussion

The observation of the scaling flows reported in section 5.2 poses the question of whether we can attribute them to the influence of a nearby renormalized trajectory and so infer the existence of a new fixed point. One interpretation of the evidence for scaling is that a new renormalized trajectory exists with exponent $\kappa \approx 4 \sim 5$, and that a new fixed point lies somewhere in the complete space of coupling constants with projection onto the (β, μ) plane of $(\beta^* \approx 7, \mu^* \approx -0.28)$. Evidence presented in section 5.3 shows that there is also a ‘vorticity’ fixed point associated with the ‘vorticity’ critical point located at about $(\beta_c \approx 7, \mu_c \approx -0.26)$ which terminates the first-order line. Because of the proximity of these two points to each other it is tempting to identify the new fixed point with the ‘vorticity’ fixed point. However, there is no direct evidence that this is so and there are

arguments against such an identification. The first is that we would expect the continuum limit defined at the ‘vorticity’ fixed point to be ising-like since the order parameter is based on a locally discrete variable: the plaquette operator, $P_{\mathbf{x}}(\sigma)$. The exponent κ for ising-like critical points is $\kappa = 8/15$ whereas for the new renormalized trajectory we find $\kappa \approx 4 \sim 5$. This is clearly inconsistent with the proposal. The second argument is that the identification of the two fixed points means that the ‘vorticity’ critical point is in the domain of attraction of the new fixed point. The consequence is that there must be a fixed point of the flows in the $(\langle A \rangle, \langle P \rangle)$ plane in the limit that the initial lattice size is large enough: $L \rightarrow \infty$. This is true because flows that have bare couplings held at the critical point values must be in the critical surface and so flow towards the new fixed point. In turn this implies that the correlation length $\xi_A(\beta, \mu)$ for a state interpolated by A must diverge at the ‘vorticity’ critical point, (β_c, μ_c) . This is unlikely since we expect $\xi_A(\beta, \mu)$ to be bounded from above by the correlation length in the $O(3)$ model at the same β , namely $\xi_A(\beta, \infty)$. This is because for $\mu < \infty$ the presence of vortices introduces disorder in the system which acts to reduce the correlation length at fixed β . However, $\xi_A(\beta, \infty)$ diverges only in the limit $\beta \rightarrow 0$, the $O(3)$ fixed point, and hence $\xi_A(\beta, \mu)$ cannot diverge at (β_c, μ_c) contradicting the proposed identification of the two fixed points. Although we did not carry out an exhaustive investigation we found no evidence for a fixed point of the $(\langle A \rangle, \langle P \rangle)$ flows from the simulations described in section 5.2.

In figure 10 we shown an artist’s impression of a possible topology of the RG flows in coupling constant space consistent with this interpretation and with the results presented in section 5. The two axes associated with the couplings (β, μ) are augmented by a third which represents all other couplings. There are two fixed points shown. One is the usual asymptotically-free $O(3)$ fixed point and the other is the new fixed point we have identified in this work. The ‘vorticity’ fixed point is not shown. The critical surface bounds the surface of first-order transitions and the two phases associated with this transition are distinguished by the vortex density being large in one phase and small in the other. The line of intersection of the first-order surface with the (β, μ) plane is the line of first-order transitions reported above. There are a number of possible continuum limits in this model, each identified with a different fixed point. A non-zero vortex density will be associated with the continuum limit taken at the critical point controlled by the ‘vorticity’ fixed point. At the new fixed point there are two relevant directions but we cannot be sure what the relevant observables are since in this scenario the action must be augmented by other couplings so that it can be tuned to lie in the critical surface and in the domain of attraction of this fixed point. However, the presence of this renormalized trajectory dominates all flows in its neighbourhood, and its influence will only be diminished if points in the critical surface are approached which are not in its domain of attraction. The example scenario of figure 10 is complicated but we have found no simpler topology consistent with the results if we demand that the scaling flows are due to a nearby RT in an extended model.

A different interpretation is that the scaling flows are due to the ghost of the Kosterlitz-Thouless renormalized trajectory in the equivalent $O(2)$, or XY ,

model. A cogent argument against a Kosterlitz-Thouless fixed point occurring in non-abelian models has been given by Hasenbusch in [?], but it was conjectured in [?] that some remnant of Kosterlitz-Thouless behaviour might nevertheless survive in models of this kind and give rise to the pseudo-scaling behaviour reported in [?]. As remarking in section 5.2 the fit to the exponent κ using equation (5.2.2) should not be taken to rule out KT behaviour in favour of conventional second-order behaviour. Indeed, the large value for κ mitigates in favour of a KT interpretation [?]. This explanation has the virtue of simplicity over the alternative picture above but it is unclear how to describe the mechanism more fully.

The deviation from scaling for the large β points for $L = 512$ in sets 1 and 2 (table 3) can be explained by noting that there is no fixed point for the $(\langle A \rangle, \langle P \rangle)$ flows and so the attempt to follow the scaling flow to larger β and into a fixed point will fail as the critical surface is approached. The conjectured renormalized trajectory dominates by virtue of its large exponent but scaling will eventually be violated as β increases towards $\beta \sim 7$.

The strong influence of the scaling flows gives rise to a cross-over effect in the flows which signals the cross-over from the vortex to the spin-wave regions of the phase diagram. For example, in pure RP^2 this occurs at about $\beta = 4.18$, $\mu = 0$. We would naturally associate this cross-over with the observed first-order line but it is clear that the strength of the effect is due to the nearby scaling flows. This would suggest that the first-order line and the scaling flows were related but, as argued above, a simple relationship is ruled out and it is unclear whether the proximity of the two features is a coincidence or not. The region in which the cross-over occurs is quite narrow and has been shown as a surface with dotted outline in figure 10. As β is increased at fixed μ through this ‘cross-over region’, the vorticity rapidly decreases from a high to low value especially in the neighbourhood of the critical surface. This effect means that the disorder also decreases rapidly and we would expect a corresponding rapid increase in the vector and tensor correlation lengths, ξ_V and ξ_T , which are deduced respectively from the correlators $G_V(\mathbf{x}, \mathbf{y})$ and $G_T(\mathbf{x}, \mathbf{y})$ defined for RP^{N-1} by

$$\begin{aligned} G_V(\mathbf{x}, \mathbf{y}) &= \langle \mathbf{S}_\mathbf{x} \cdot \mathbf{S}_\mathbf{y} \rangle_c , \\ G_T(\mathbf{x}, \mathbf{y}) &= \langle (\mathbf{S}(\mathbf{x}) \cdot \mathbf{S}(\mathbf{y}))^2 \rangle - 1/N , \end{aligned} \quad (6.1)$$

Because G_V is not gauge invariant it will vanish unless it is evaluated in a fixed gauge. This is analogous to the situation in QED where the electron propagator is not gauge invariant but the pole mass is. Technically, the gauge-fixed electron propagator has a cut whose discontinuity is a gauge-dependent function of α but whose branch point defines the gauge-invariant mass. This is due to the continuous nature of the gauge group which does not apply in our case. A reasonable gauge choice would be to maximize $\sum_{\mathbf{x}, \boldsymbol{\mu}} \sigma_{\mathbf{x}, \boldsymbol{\mu}}$. G_T takes the same form as the tensor correlator defined by Caracciolo et al. [?] and Sokal et al. [?]. Because G_T is gauge-invariant it does not require gauge-fixing before evaluation. When the vorticity is vanishingly small the gauge field is equivalent to a pure gauge and can be gauge transformed to the trivial configuration $\sigma_{\mathbf{x}, \boldsymbol{\mu}} = 1$, $\forall \mathbf{x}, \boldsymbol{\mu}$. The physical observables in the theory are then insensitive to the chemical potential

μ and the theory is in the universality class of the $O(3)$ fixed point.

In the $O(3)$ continuum limit both ξ_V and ξ_T will diverge, but in the continuum limit defined by the vorticity fixed point we expect both ξ_V and ξ_T to remain finite because, as already discussed above, the presence of disorder means that they will be bounded from above respectively by $\xi_V(\beta, \infty)$ and $\xi_T(\beta, \infty)$, the correlation lengths at the same value of β in the $O(3)$ spin model. In other words, at fixed β we expect both ξ_V and ξ_T to increase as μ increases, achieving their maximum values at $\mu = \infty$ in the $O(3)$ model. This increase could be very rapid in the vicinity of the cross-over region. The operators interpolating the states in G_V and G_T are, respectively, $V_i = S_i$ and $T_{ij} = S_i S_j - 1/N \delta_{ij}$. Since $\langle V_i \rangle = \langle T_{ij} \rangle = 0$ they show no discontinuity across the first-order line and hence ξ_V and ξ_T will not diverge at the critical point terminating the first-order line (gauge fixing is understood where necessary). If either of ξ_V or ξ_T did diverge it would contradict the expectation that they are bounded from above by their corresponding values in $O(N)$ as mentioned above. In principle, we could also study $G_S(\mathbf{x}, \mathbf{y}) = \langle U_C(\mathbf{x}) U_C(\mathbf{y}) \rangle_c$ since $\langle U_C \rangle$ is continuous across the first-order line and it couples to the S-wave two-particle $O(N)$ singlet state. The associated correlation length ξ_S should coincide with ξ_T in the continuum limit if the conventional scenario is assumed. We suggest that the divergent correlation length at the critical point is associated with the correlator of $U_D(\mathbf{x})$, or equivalently with the vorticity correlator

$$G_P((\mathbf{x}, \mathbf{y})) = \langle P_{\mathbf{x}} P_{\mathbf{y}} \rangle. \quad (6.2)$$

In this study G_P was not computed.

The pure RP^2 model ($\mu = 0$) does not intersect any critical surface except the one in the basin of attraction of the $O(3)$ fixed point at $\beta = \infty$. This confirms the conjectures of Niedermayer et al. [?] and Hasenbusch [?] that RP^2 and $O(3)$ have the same continuum limit. In a simulation of pure RP^2 Kunz and Zumbach [?] observe the rapid decrease in vorticity that we have associated with the cross-over region, and Niedermayer et al. [?] comment that in this region a sharp transition to a huge value for ξ_V is to be expected. Our result is that the cross-over is very strongly marked in the renormalized quantities obtained after substantial blocking has been performed. The cross-over region separates two phases in one of which the vorticity density is high with a background of vortices pairs overlaid by a gas of free vortices, and in the other the vorticity density is low and does not scale as $\beta \rightarrow \infty$. These two phases are also separated by a first-order line and we conjecture that a non-zero scaling limit for the vortex density could exist at the terminating critical point. Huang and Polonyi [?] have discussed the existence of a continuum limit with a non-zero scaling vorticity in a generalized 2D Sine-Gordon model and the non-conservation of the kink current. A similar analysis could be fruitful in non-abelian models of the kind discussed in this paper, although it is unclear if the same techniques are directly applicable.

In the simulation of the 2D $SO(4)$ matrix model [?] a bogus signal for scaling was observed which led to an incorrect measurement of the $m/\Lambda_{\overline{MS}}$ ratio. In the context of RP^2 we would expect a similar effect for $\beta \sim 3.9$ because in this case the model renormalizes close to the scaling flows and so in the neighbourhood of

this coupling we should expect to see a good scaling signal. The effect is enhanced by the large exponent $\kappa \sim 4$ associated with these flows. Simulations which are designed to compute $m/\Lambda_{\overline{MS}}$ must have $\xi_V \ll L$ for some largest practical lattice size, L . Because ξ_V is rising rapidly in this region as a function of β , this means that only a small range of β is useable and that this range corresponds to theories where the vorticity is not too low since ξ_V would otherwise already be too large. The conclusion is that such simulations will see an apparent scaling due to the strong influence of the scaling flows. However, this scaling is not a signal for a continuum limit in pure RP^2 but is due to the proximity of the cross-over region to the scaling flows. On much larger lattices as β is increased a cross-over to true scaling would eventually be observed: the scaling associated with the $O(3)$ fixed point. However, this would be for prohibitively large values of ξ_V , perhaps as large as $\xi_V \sim 10^9$ [?]. We believe that this effect explains the results presented in [?] who observe scaling in RP^2 (RP^3) but who find that the observed correlation length is smaller by a factor of 10^7 (10^4) than that deduced assuming that the theory is asymptotically free. We suggest that this study is actually in the cross-over regime where the correlation length is diminished by the disordering effect of vortices and the scaling, which is perhaps due to a new renormalized trajectory, is only apparent. The true scaling regime associated with the $O(3)$ ($O(4)$) fixed point will correspond to much larger correlation lengths than those studied. We believe that a similar effect caused the bogus signal for scaling in the analysis of the $SO(4)$ matrix model [?] and the mismatch between the observed mass-gap and the Bethe-Ansatz prediction.

We conclude that the RP^2 and $O(3)$ spin models are in the same universality class and that there is no evidence to the contrary. This confirms the conclusions of Hasenbusch [?] and Niedermayer et al. [?], but is at variance with the proposition of Caracciolo et al. [?] that the continuum limits of these two models are distinct. These latter authors propose that there is a continuous set of universality classes in a 2D model with mixed isovector and isotensor $O(3)$ spin interactions. The $O(3)$ and RP^2 theories correspond to the pure isovector and pure isotensor interactions respectively, and the proposition of Caracciolo et al. requires that these two models be in different universality classes. The work presented in this paper shows that the opposite is true and hence that the existence of a continuous set of universality classes in the mixed model is unlikely.

7 Conclusions

In this paper we have studied the 2D RP^2 gauge model that is characterized by two couplings (β, μ) , where μ is the chemical potential controlling the vorticity computed from the gauge field plaquette expectation value. We have found that the rôle played by the vorticity in the nature of the phase diagram is crucial. Using standard methods we confirm the existence of a first-order transition (figures 5 to 7), first suggested by Solomon et al. [?], in the (β, μ) plane separating phases of high and low vorticity. The critical point terminating this first-order line is established to lie in the range $7.0 < \beta_c < 7.5$, $\mu_c \sim -0.26$, which implies the existence of a ‘vorticity’ fixed point controlling the continuous transition at

(β_c, μ_c) . We use the Monte-Carlo renormalization group for blocking the spin-spin interaction and plaquette expectation values, $\langle A \rangle$ and $\langle P \rangle$, to investigate the topology of the renormalization group flows. We verify the presence of the $O(3)$ -renormalized trajectory (at $\mu = \infty$) and find results consistent with the known three-loop β -function for sufficiently large β once the finite lattice-spacing artifact has been taken into account. We establish the existence of new scaling flows in the $(\langle A \rangle, \langle P \rangle)$ plane (figures 3 and 4) and conjecture that they are due either to the ghost of the Kosterlitz Thouless renormalized trajectory in the XY model or to a new renormalized trajectory and its associated fixed point which should lie out of the (β, μ) plane in the complete space of couplings. The scaling flows are consistent with a critical exponent $\kappa \approx 4 \sim 5$ and the projection of the conjectured fixed point onto the (β, μ) plane is deduced to be in the range $\beta^* \approx 6.5 \sim 7.5$, $\mu^* \approx -0.31 \sim -0.26$. Although the values of (β_c, μ_c) and (β^*, μ^*) are very similar there are strong arguments against identifying the conjectured fixed point with the ‘vorticity’ fixed point. One is that the exponent κ is much larger than that expected at the ‘vorticity’ fixed point, and another is that such an identification would imply a fixed point in the $(\langle A \rangle, \langle P \rangle)$ flows for bare couplings (β_c, μ_c) , with a consequent divergence in certain correlation lengths. This is contradicted by the fact that, because of the presence of non-zero vorticity, these correlation lengths are bounded from above by the corresponding quantities in the $O(3)$ model ($\mu = \infty$) at the same β which are known not to diverge for $\beta < \infty$. A consequence is that the critical point at (β_c, μ_c) cannot be in the domain of attraction of the conjectured fixed point. The scaling flows dominate the flows in their vicinity and in particular gives rise to a cross-over (figures 6 and 7) between regions of high vorticity (lower β) to low vorticity (higher β) associated by a rapid increase in the correlation length as the disorder is reduced. We conclude that simulations in the neighbourhood of the cross-over region for $\mu > -0.26$ will show ‘pseudo’ scaling [?] because of the proximity of these scaling flows. The true continuum limit for such models will not be observed until true scaling, controlled by the $O(3)$ fixed point, has been established at larger β and very much larger correlation length. This is the case for the RP^2 spin model ($\mu = 0$) whose continuum limit is controlled by the $O(3)$ fixed point and which is thus in the same universality class as $O(3)$, contradicting Caracciolo et al. [?] but confirming the work of Hasenbusch [?] and Niedermayer et al. [?]. It also gives an explanation for the results discussed by Caracciolo et al. [?]. In figure 10 an artist’s impression of the renormalization group flows is given for one scenario consistent with our results. The natures of any new fixed points are not established because of the known difficulty [?] in distinguishing between fits of different scaling forms and the compatibility of the observed scaling with a second-order scaling form, equation (5.2.2) is of phenomenological significance only. It is quite possible that any fixed point whose existence we infer from the data is of Kosterlitz-Thouless type.

Our investigation has shown that the nature of gauged spin models is complicated and it is difficult to pin down more about the nature and location of the topological features of the renormalization group flows without more information concerning the relevant operators in each case. However, it is clear that a fixed

point in a larger coupling constant space can be close enough to the subspace of simple models that it very strongly influences observables and the outcome of tests for scaling in exactly that region accessible by simulation, namely for those couplings for which the correlation lengths have increased to the practical limit measurable on modern computers. This influence is strengthened if the exponent of the associated renormalized trajectory is large. The model studied in this paper is a good example of this effect.

It would be interesting to more accurately locate the critical point at (β_c, μ_c) terminating the first-order line and investigate the continuum limit it defines.

8 Acknowledgements

This work is supported by NATO collaborative research grant no. CRG950234. The authors wish to thank Ian Drummond for useful conversations. The computing resources were provided by the High performance Computing Centre, University of Cambridge and by the Computer Centre, University of Tokyo.

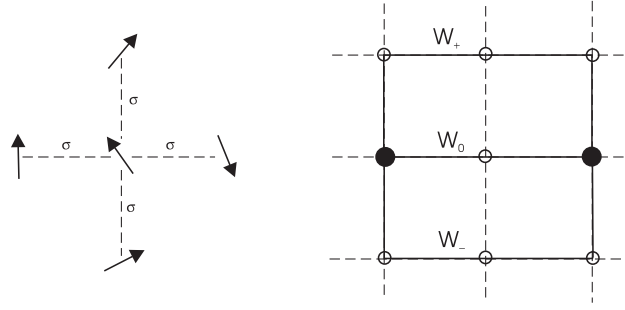


Figure 1: Blocking strategies for spins and gauge fields. A gauge-covariant linear combination of a spin and its nearest neighbours defines the blocked spin and the gauge field on the blocked link, which connects the solid-black sites, is assigned the majority sign of the three Wilson lines W_+ , W_0 , W_- .

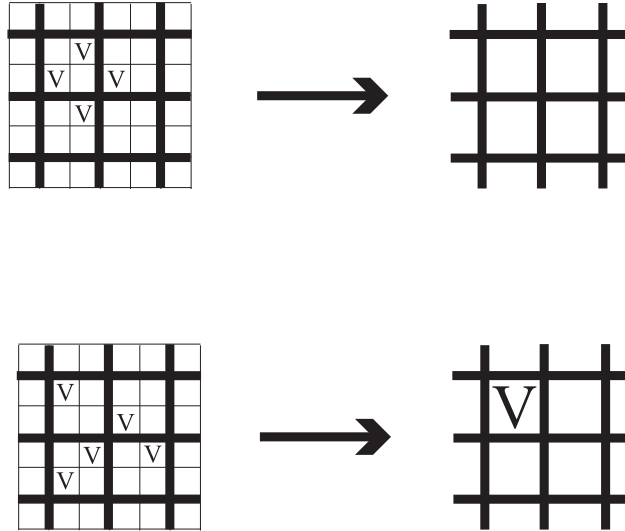


Figure 2: The results of example blocking of two vortex configurations. Since vortices add mod_2 the blocking should yield either no blocked vortices or one blocked vortex depending on whether the original region contained an even or odd number of vortices. The majority rule of equation (4.40) guarantees this important property.

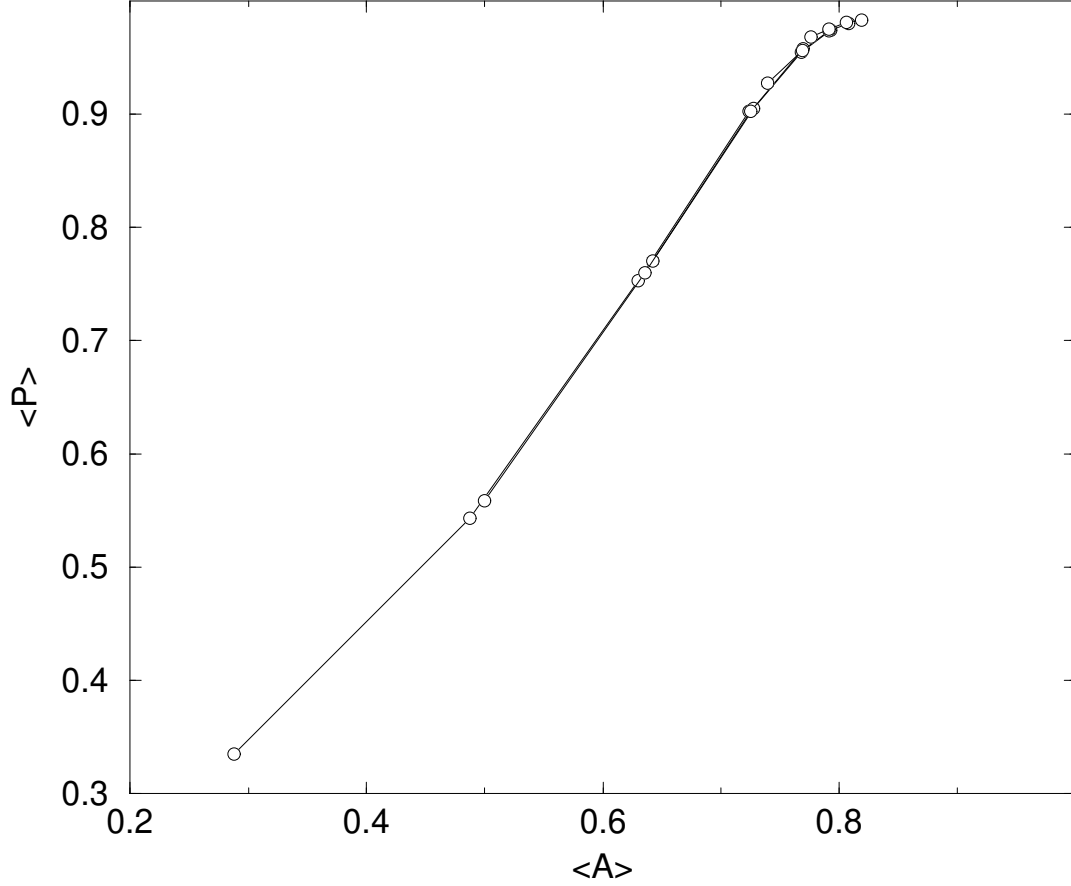


Figure 3: The scaling flow built up from the RG flow segments of set1 given in table 3. Each segment consists of four points corresponding to the $(\langle A \rangle, \langle P \rangle)$ values on an $L = 8$ lattice blocked for given couplings from lattices with $L = 64, 128, 256, 512$, respectively. The segments are adjusted so that they overlay each other, and it can be seen from this figure, and from table 3, that the points on different segments coincide very well indicating that scaling holds. There are two errant points corresponding to the two largest β values and $L = 512$.

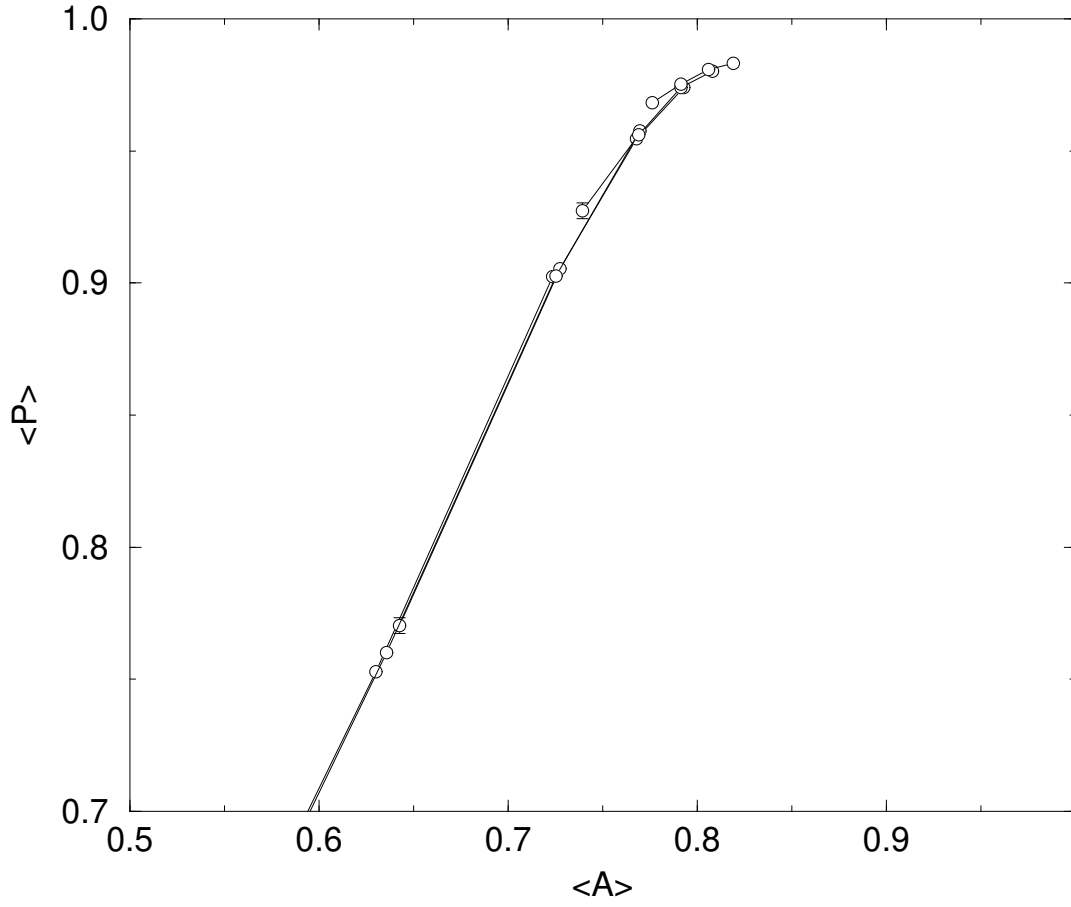


Figure 4: Detail of figure 3. Caption as for figure 3

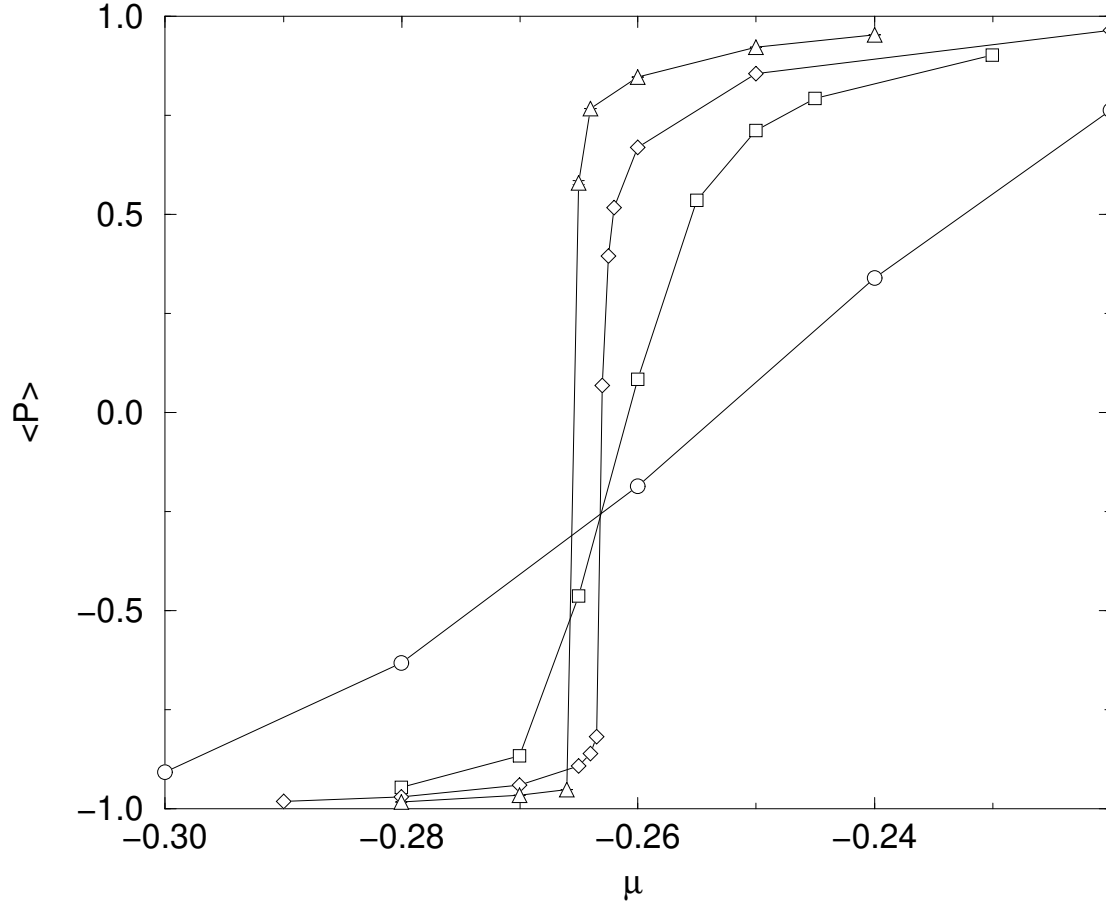


Figure 5: $\langle P \rangle$ defined by eq. 4.1 as a function of μ for $\beta = 6.0$ (\circ), 7.0 (\square), 7.5 (\diamond), 8.0 (\triangle) .

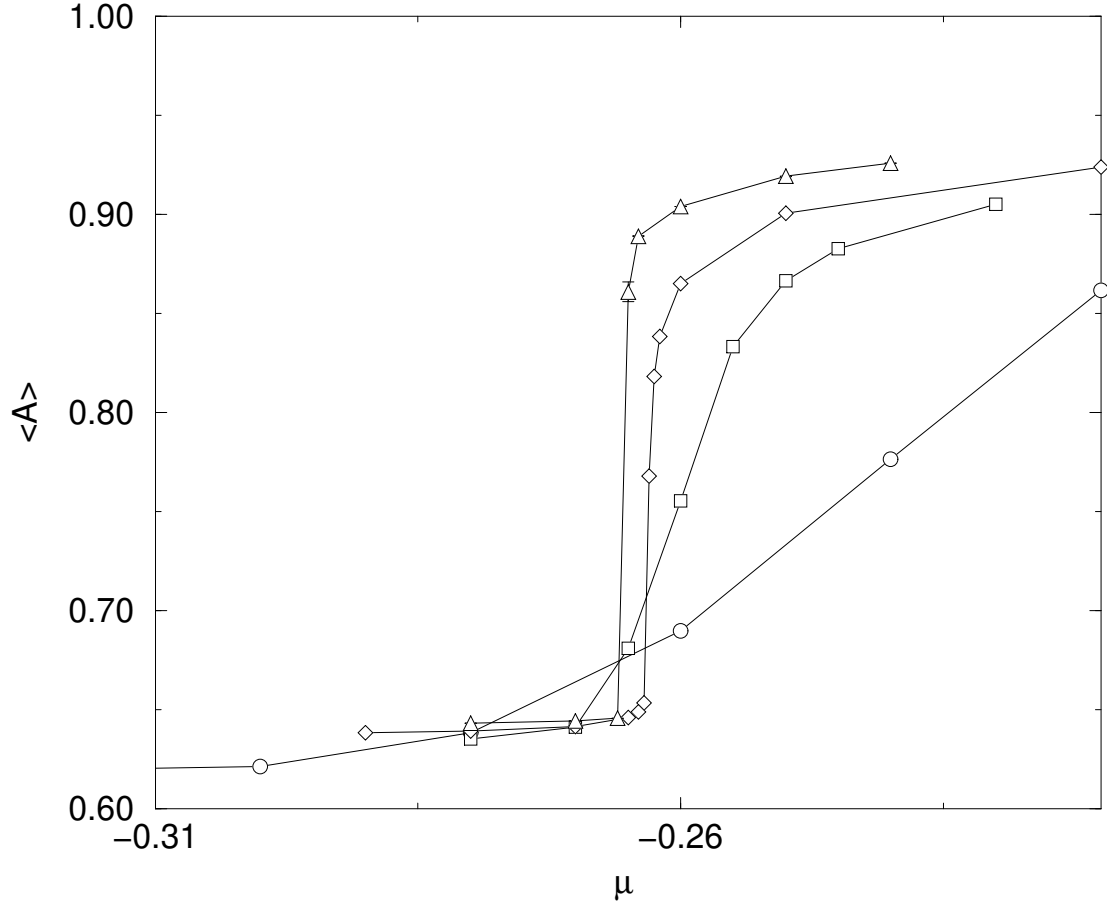


Figure 6: $\langle A \rangle$ defined by eq. 4.1 as a function of μ for $\beta = 6.0$ (\circ), 7.0 (\square), 7.5 (\diamond), 8.0 (\triangle) .

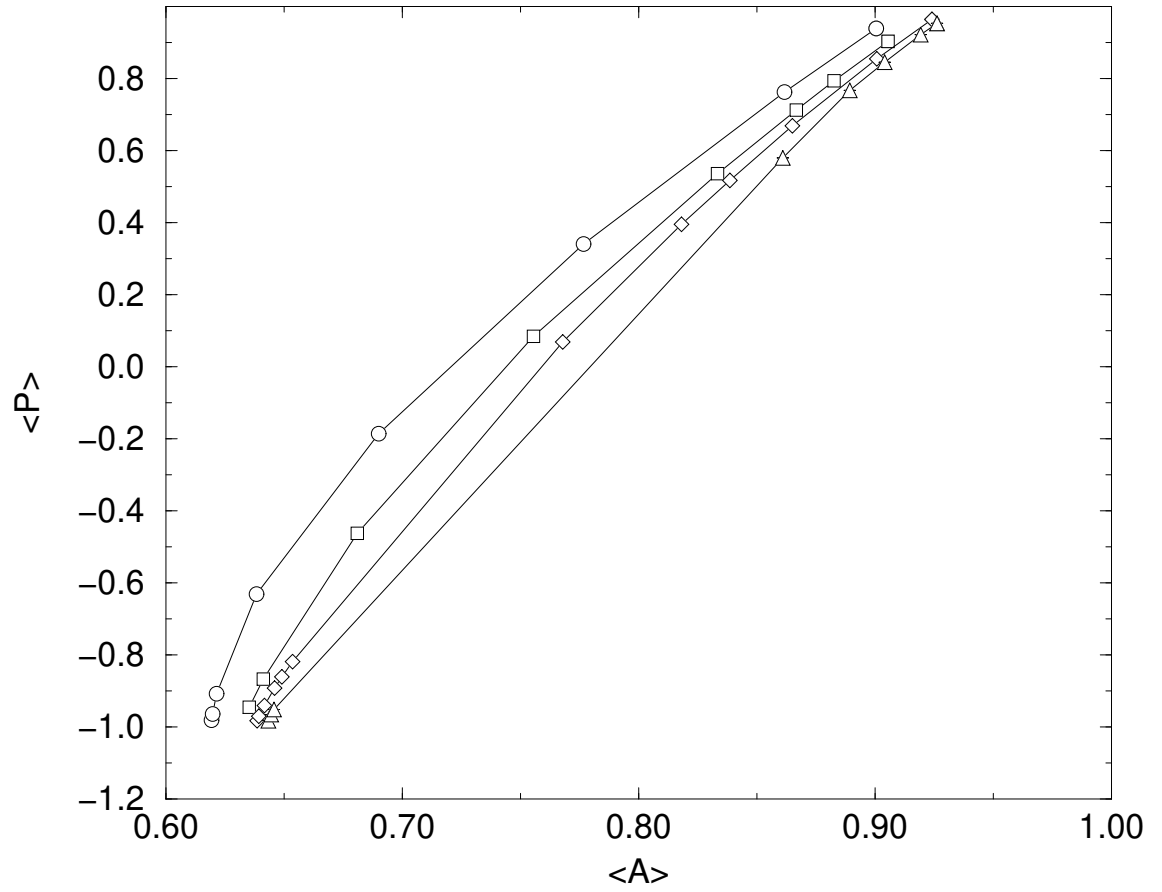


Figure 7: $\langle A \rangle$ versus $\langle P \rangle$, defined by eq. 4.1, for $\beta = 6.0$ (\circ), 7.0 (\square), 7.5 (\diamond), 8.0 (\triangle) .

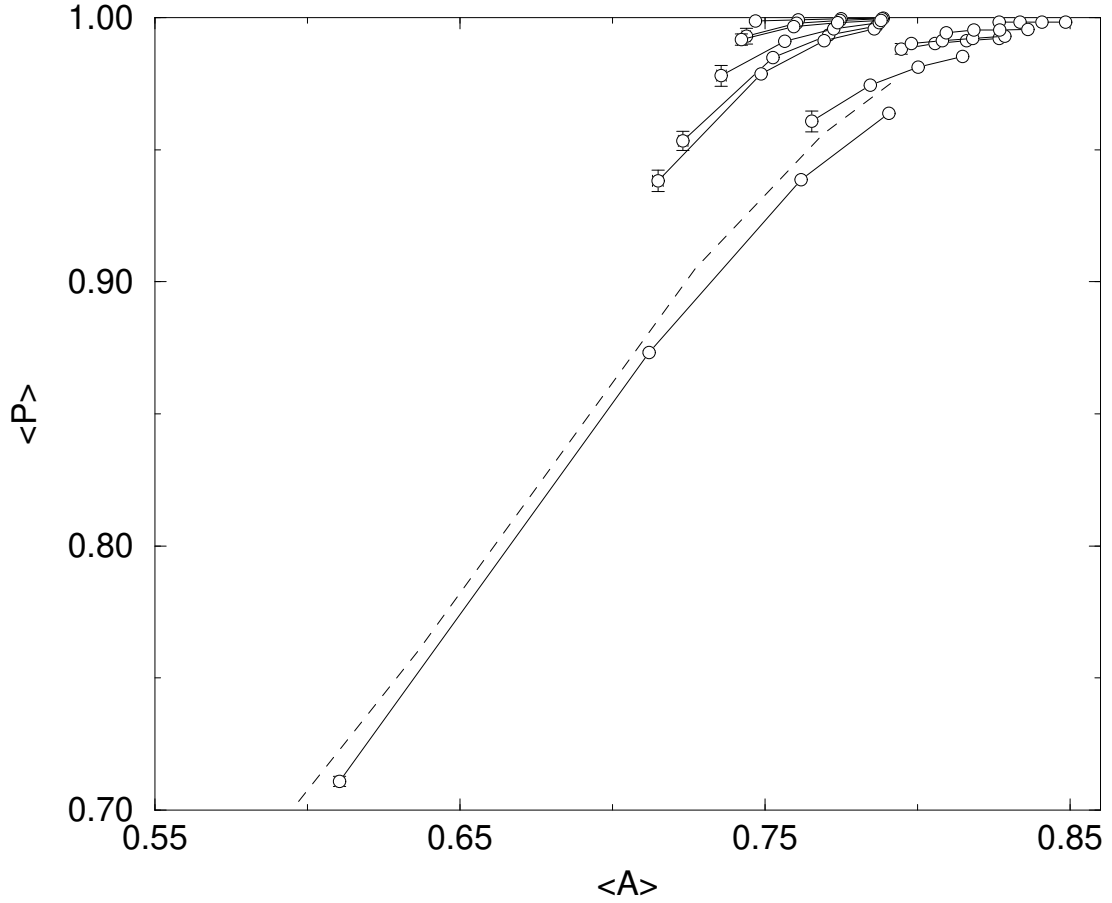


Figure 8: Two examples sets of flows, sets 3 and 4, showing cross-over of flows. Set 3 lies to the left of set 4 and the (β, μ) values corresponding to these sets are given in table 5. Set 4 is for various β in the RP^2 model ($\mu = 0$) in the range $\beta = 3.9$ to 4.5. There is rapid variation in the renormalized $(\langle A \rangle, \langle P \rangle)$ values for small changes in β indicating a narrow cross-over from a region of high to low renormalized vorticity. For $\beta \sim 4$ the RP^2 flows closely follow the scaling flow of figure 3, shown here as the dashed curve, implying scaling will apparently hold until, for larger β , the cross-over occurs.

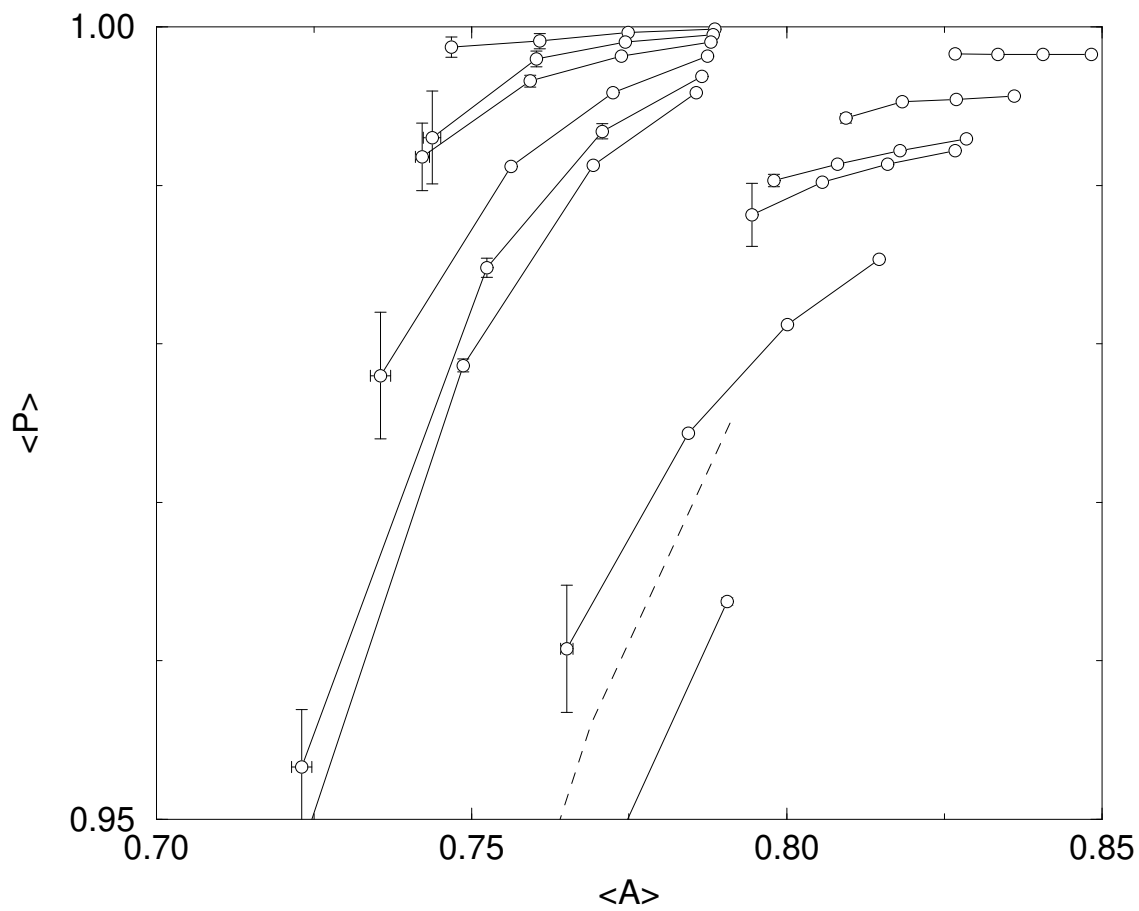


Figure 9: Detail of figure 8. Caption as for figure 8

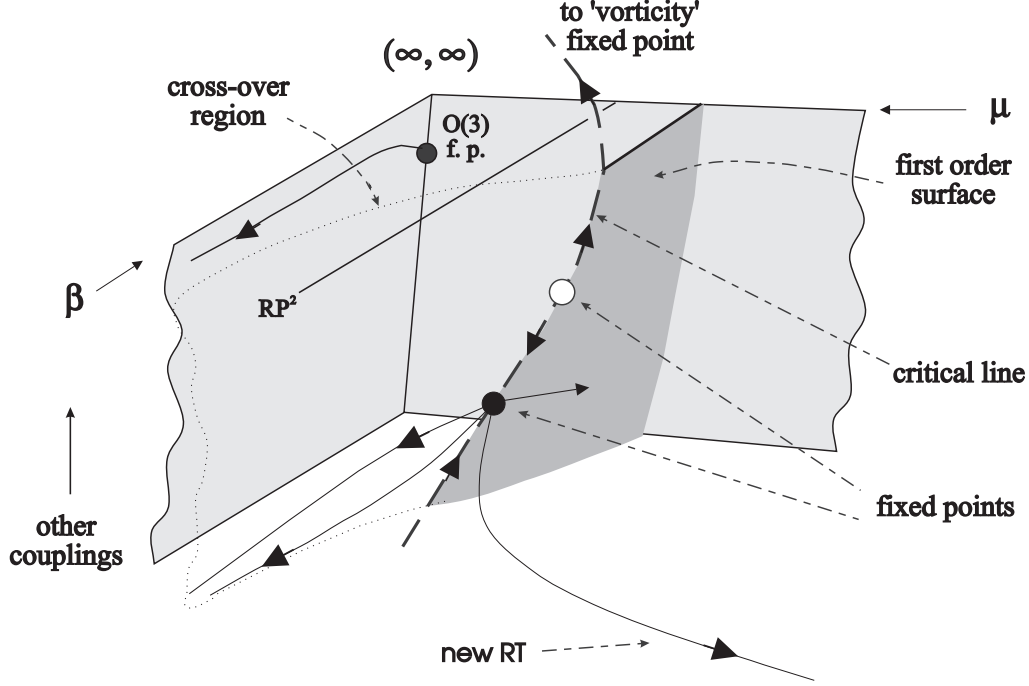


Figure 10: An artist's impression of the RG flows consistent with the simulation results. The $O(3)$ fixed point controls the continuum limit of RP^2 ($\mu = 0$) and neighbouring theories. A line of critical points terminates the first-order surface and defines new continuum limits characterized by non-zero continuum vorticity. The observed renormalized trajectory is shown associated with a new fixed point in the critical surface. There are indications that this fixed point does not control the second-order transition terminating the observed first-order line in the (β, μ) plane, and the scenario presented here is consistent with this view. The cross-over region is the neighbourhood of the surface shown with dotted outline.